We are IntechOpen,
the world's leading publisher of
Open Access books
Built by scientists, for scientists

6,900
Open access books available

185,000
International authors and editors

200M
Downloads

154
Countries delivered to

Our authors are among the

TOP 1%
most cited scientists

12.2%
Contributors from top 500 universities

CLARIVATE ANALYTICS

**BOOK
CITATION
INDEX**

INDEXED

WEB OF SCIENCE™

Selection of our books indexed in the Book Citation Index
in Web of Science™ Core Collection (BKCI)

Interested in publishing with us?
Contact book.department@intechopen.com

Numbers displayed above are based on latest data collected.
For more information visit www.intechopen.com

Enhanced Boiling Heat Transfer from Micro-Pin-Finned Silicon Chips

Jinjia Wei and Yanfang Xue
Xi'an Jiaotong University
China

1. Introduction

A computer is mainly composed of chips on which a large number of semiconductor switches are fabricated. The requirement for increasing signal speed in the computer has focused the efforts of electronics industry on designing miniaturized electronic circuits and highly integrated circuit densities in chips. The integration technologies, which have advanced to the very large scale integration (VLSI) level, lead to an increased power dissipation rate at the chip, module and system levels. Sophisticated electronic cooling technology is needed to maintain relatively constant component temperature below the junction temperature, approximately 85°C for most mainframe memory and logic chips. Investigations have demonstrated that a single component operating 10°C beyond this temperature can reduce the reliability of some systems by as much as 50% (Nelson, 1978).

Traditionally, convection heat transfer from electronic hardware to the surroundings has been achieved through the natural, forced, or mixed convection of air; however, even with advances in air-cooling techniques, the improvements will not suffice to sustain the expected higher heat fluxes. As an effective and increasingly-popular alternative to air cooling, directly immersing the component in inert, dielectric liquid can remove a large amount of heat dissipation, of which pool and forced boiling possess the attractive attribute of large heat transfer coefficient due to phase change compared with single-phase.

An ideal boiling performance should provide adequate heat removal within acceptable chip temperatures. Direct liquid cooling, involving boiling heat transfer, by use of dielectric liquids has been considered as one of the promising cooling schemes. Primary issues related to liquid cooling of microelectronics components are mitigation of the incipience temperature overshoot, enhancement of established nucleate boiling and elevation of critical heat flux (CHF). Treated surface has been found to have great potential in enhancement of boiling heat transfer from electronic, significantly reducing the chip surface temperature and increasing CHF. Treated surfaces are used for nucleate boiling enhancement by applying some micro-structures on the chip surface to make the surface capable of trapping vapour and keeping the nucleation sites active or increasing effective heat transfer area. Since the 1970s, a number of active studies have dealt with the enhancement of boiling heat transfer from electronic components by use of surface microstructures that were fabricated directly on a silicon chip or on a simulated chip. These include a sand-blasted and KOH treated surface (Oktay 1982), a "dendritic heat sink" (brush-like structure) (Oktay and

Schemekenbecher 1972), laser drilled cavities (3-15μm in mouth dia.) (Hwang and Moran 1981), re-entrant cavities (0.23-0.49 mm in mouth dia.) (Phadke et al. 1992).

Messina and Parks (1981) used flat plate copper surfaces sanded with 240 and 600 grit sandpaper to boil R-113 and found the sandpaper finished surfaces were very efficient in improving boiling heat transfer and elevating CHF as compared to a smooth surface, with 240 grit more efficient than 600 grit. Anderson and mudawar (1989) roughened a 12.7-mm square copper surface by longitudinal sanding with a 600 grit silicon wet/dry sand paper to examine the effect of roughness on boiling heat transfer of FC-72. The roughness was 0.6-1.0 μm and the roughened surface produced an earlier boiling incipience than smooth surface and shifted the boiling curve toward a reduced wall superheat. However, the CHF value was not affected by the roughness as compared with the results obtained by Messina and Parks (1981). Chowdhury and Winterton (1985) found nucleate boiling heat transfer improved steadily as the surface roughness level was increased. However, when they anodized a roughened surface covered with cavities of around 1 μm size, which had hardly any effect on the roughness, they observed that the nucleate boiling curves were virtually independent of roughness. They asserted that it was not roughness in itself but the number of active nucleation sites that influenced nucleate boiling heat transfer.

Oktay and Schmeckenbecher (1972) developed a brush-like structure called "dendritic heat sink" mounted on a silicon chip surface, and the thickness of the dendrite was 1 mm. The incipience boiling temperature in saturated FC-86 could be reduced to 60°C due to the high density of re-entrant and possibly doubly re-entrant cavities provided by the dendritic heat sinks, and an increase in CHF compared with a smooth surface was attributed, by the authors, to the deferred creation of Taylor instability on the dendritic surface.

Chu and Moran (1977) developed a laser-treated surface on a silicon chip, which consisted of drilling an array of cavities ranging in average mouth diameter from 3 to 15 μm staggered 0.25-mm centers. Boiling data in FC-86 revealed that the wall superheat at any particular heat flux decreased, and the critical heat flux was increased by 50%.

Phadke et al. (1992) used a re-entrant cavity surface enhancement for immersion cooling of silicon chip. The pool boiling heat transfer characteristics of the cavity enhanced surfaces were superior to those of a smooth surface, resulting in a substantial decrease in both the temperature overshoot and the incipient boiling heat flux.

Kubo et al. (1999) experimentally studied boiling heat transfer of FC-72 from micro-reentrant cavity surfaces of silicon chips. The effects of cavity mouth size (about 1.6μm and 3.1μm) and the cavity number density (811/cm² and 9600/cm²) were also investigated. The heat transfer performance of the treated surface was considerably higher than that of the smooth surface. The highest performance was obtained by a treated surface with larger cavity mouth diameter and cavity number density.

Nakayama et al. (1982) developed a tunnel structure, in which parallel rectangular cross-sectional grooves with the dimensions of 0.25×0.4 mm² (width×depth) were firstly gouged with a pitch of 0.55 mm on a copper surface (20×30 mm²), then covered by a thin copper plate having rows of 50-to-150 μm diameter pores. R-11 was boiled and the wall superheat was reduced as compared to a smooth surface. They attributed the boiling enhancement to the liquid suction and evaporation inside the grooves. Later, Nakayama et al. (1989) used a 5-mm high porous copper stud with micro-channels to enhance boiling heat transfer of dielectric fluid FC-72. The porous stud could reduce the threshold superheat for the boiling

incipience and increasing CHF. The boiling heat transfer levelled off with further increasing stud height.

Anderson and Mudawar (1989) also attached mechanically manufactured cavities, micro-fins and micro-pin-fins to vertical 12.7 mm square copper chips immersed in a stagnant pool of FC-72. They found that large artificial cavities with the mouth diameter of 0.3 mm were incapable of maintaining a stable vapour embryo and had only a small effect on boiling heat transfer compared with a smooth surface, while micro-finned and micro-pin-finned surfaces significantly enhanced the nucleate boiling mainly due to a heat transfer area increase. The micro-pin-finned surface with the fin dimensions of 0.305×0.305×0.508 mm^3 (width×thickness×height) provided CHF values in excess of 50 W/cm^2 and 70 W/cm^2 for the liquid subcoolings of 0 and 35K, respectively.

In 1990's, You and his co-researchers made a noticeable progress in nucleate boiling enhancement by use of a series of micro-porous surfaces. You et al. (1992) applied a 0.3-3.0 μm alumina particle treatment on a simulated electronic chip surface with spraying method and tested in FC-72. Compared with a smooth reference surface, a reduction of 50% in incipient and nucleate boiling superheats and an increase of 32% in the CHF were realized. O'Connor and You (1995) further used the spraying application to apply the alumina particles (0.3-5.0 μm) on a simulated electronic chip surface. The enhancement of nucleate boiling heat transfer showed excellent agreement with those observed by You et al. (1992) with an exception of a much higher CHF increase (47% increase) due to the increased heater thickness (1 mm aluminium nitride) which provided CHF data free from thermal conductance/capacitance effects.

In their subsequent studies, O'Connor and You (1995), O'Connor et al. (1996) painted 3-10μm silver flakes or 8-12 μm diamond particles on the copper surface. Chang and You (1996, 1997) used 1-50μm copper particles and 1-20 μm aluminium particles to form porous coatings. These micro-porous coating surfaces showed almost identical high boiling enhancement with a reduced incipient superheat, increased nucleate boiling heat transfer coefficient and CHF as compared to an unenhanced surface. These performance enhancements were due to the creation of micro-porous structures on the heater surfaces which significantly increased the number of active nucleation sites.

Bergles and Chyu (1982) reported a pool boiling from a commercial porous metallic matrix surface. Working fluids were R-113 and water. The excellent steady boiling characteristics of this type of surface were confirmed, however, high wall superheat were required in most cases to initiate the boiling. From the previously mentioned investigations, it is apparent that surface microstructure of the correct size plays an important role in the enhancement of boiling heat transfer. Most treated surfaces can reduce the boiling incipience temperature, improve the nucleate boiling heat transfer and increase CHF. However, the enhancement often deteriorated greatly in the high heat flux region, especially near CHF resulting in a too high wall temperature at the CHF point as compared to the maximum allowable temperature for the normal operation of LSI chips, making the enhancement not so sound in practical high-powered electronics cooling application.

Mudawar's group (Ujereh et al. 2007) studied the nucleate pool boiling enhancement by use of carbon nanotube (CNT) arrays, and found CNTs were quite effective in reducing incipience superheat and enhancing the boiling heat transfer coefficient.

Li et al. (2008) reported a well-ordered 3D nanostructured macroporous surfaces which was fabricated by elecrodeposition method for efficiently boiling heat transfer. Since the

structure is built based on the dynamic bubbles, it is perfect for the bubble generation applications such as nucleate boiling. The result indicated that at heat flux of 1W/cm², the heat transfer coefficient is enhanced over 17 times compared to a plain reference surface.

El-Genk and Ali (2010) experimentally studied the enhancement of saturation boiling of degassed PF-5060 dielectric liquid on microporous copper dendrite surfaces. These surface layers were deposited by electrochemical technique. The result showed that the thickest layer (145.6μm) of Cu nanodendrite surface is very promising for cooling electronic components, while keeping the junction temperature relatively low and no temperature excursion.

However, it is still a challenge for these treated surfaces to increase CHF by a large margin for the application of cooling with high-heat-flux chip.

The present work is to develop a surface treatment that can provide a nearly invariant high heat transfer rate throughout the whole nucleate boiling region and elevate CHF greatly within an acceptable chip temperature. For the previous micro structured surfaces, the reason for the severe deterioration of heat transfer performance at high heat fluxes is that a large amount of vapors accumulate in the structures which prevent the bulk of liquid from contacting the superheated wall for vaporization. The enhancement, due to the increased thermal resistance of the large amount of vapours trapped in the microstructures, tapers off noticeably as the heat flux approaches the CHF (See Fig. 1).
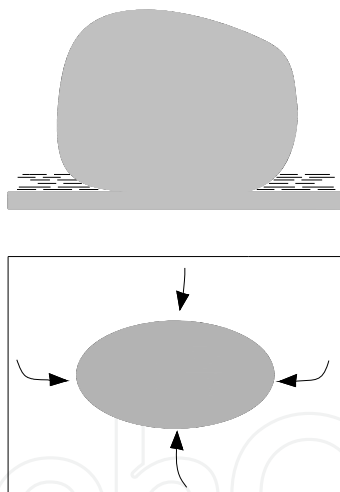

Fig. 1. Schematic of heat transfer phenomenon of smooth or previous porous structures

Therefore, the high-efficiency microstructures should provide a high driving force and a low-resistance path for the easy access of bulk liquid to the heater surface despite of large bubbles covering on the surface at high heat fluxes. Subsequently, Wei et al. (2003) developed a new model for the heat transfer and fluid flow in the vapour mushroom region of saturated nucleate pool boiling. The vapour mushroom region is characterized by the formation of a liquid layer interspersed with numerous, continuous columnar vapour stems underneath a growing mushroom-shaped bubble shown in Fig. 2. And, the liquid layer between the vapour mushroom and the heater surface has been termed as the macrolayer, whereas the thin liquid film formed underneath vapour stems is known as the microlayer. Thus, three highly efficient heat transfer mechanisms were proposed in Wei et al. (2003)'s

model, which regards the conduction and evaporation in the microlayer region, the conduction and evaporation in the macrolayer region and Marangoni convection in the macrolayer region as the heat transfer mechanism. Furthermore, Wei et al. (2003)'s numerical results showed that the heat transfer can be efficiently transferred to the vapour-liquid interface by the Marangoni convection. At the same time, the evaporation at the triple–point (liquid-vapour-solid contact point) plays a very important role in the heat transfer with a weighting fraction of about 60% over the heat flux ranges investigated, and the relative evaporations at the bubble-liquid interface and the stem-liquid interface are about 30% and 10% respectively. However, the vapour stem will eventually collapse and result in shut off of the Marangoni convection and microlayer evaporation in the vapour mushroom region of saturated pool nucleate boiling heat transfer. On the above situation, further investigations were also carried out by Wei et al. (2003) for the cases in which Marangoni convection or/and microlayer evaporation were not considered. The result indicated that the highest wall temperature can be obtained in the cases of no Marangoni convection and microlayer evaporation. So, this indicates that both the Marangoni convection and microlayer evaporation play important roles in the mushroom region of saturated pool nucleate boiling heat transfer.
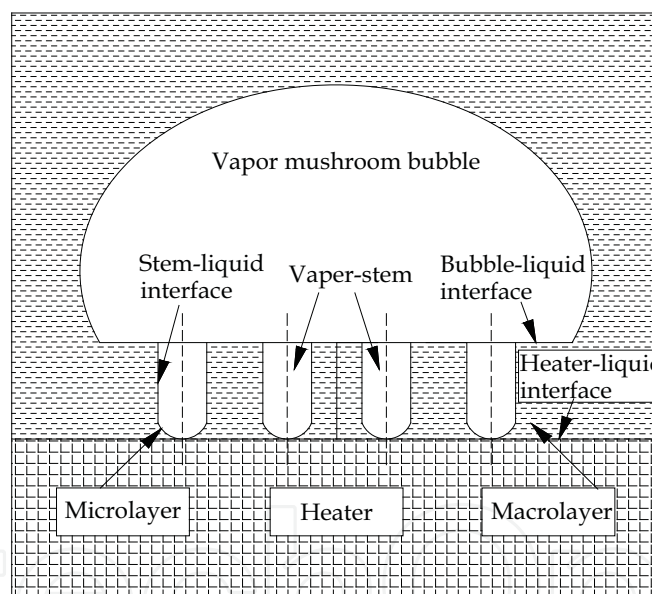

Fig. 2. Schematic of vapour mushroom structure near heated surface

Therefore, to overcome the above problems occur, we developed a micro-pin-finned surface with the fin thickness of 10-50 μm and the fin height of 60-120 μm. The fin gap was twice the fin thickness. The generated bubbles staying on the top of the micro-pin-fins can provide a capillary force to drive plenty of fresh liquid into contact with the superheated wall for vaporization through the regular interconnected structures formed by micro-pin-fins, as well as improve the microlayer evaporation and the Marangoni convection heat transfer by the motion of liquid around the micro-pin-fins (See Fig. 3).

So, the boiling heat transfer performance of FC-72 for the micro-pin-finned surfaces was firstly carried out in pool boiling test system. The maximum cooling capacity of this type of cooling module is determined by either the occurrence of CHF or complete vapor-space

condensation (Kitching et al.1995). Then, some researchers such as Mudawar and Maddox (1989), Kutateladze and Burakov (1989), Samant and Simon (1989), and Rainey et al. (2001), have found that both of fluid velocity and subcooling had significant effects on the nucleate boiling curve and the critical heat flux of their thin film heater. Therefore, the combined effects of fluid velocity and subcooling on the flow boiling heat transfer of FC-72 over micro-pin-fined surfaces were investigated for further enhancement of boiling heat transfer to cool high-heat-flux devices.
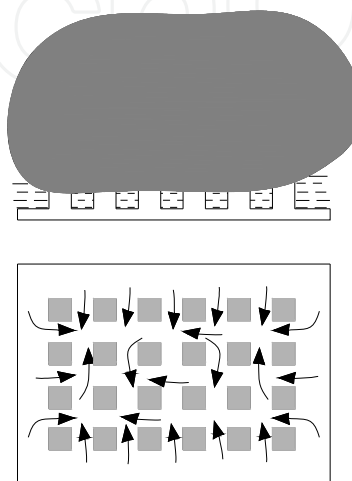
Fig. 3. Schematic of boiling heat transfer phenomena of micro-pin-fins at high heat flux near CHF

2. Experimental apparatus and procedure

2.1 Test facility of pool boiling

The first test facility for pool boiling heat transfer is shown schematically in Fig. 4. The test liquid FC-72 was contained within a rectangular stainless vessel with an internal length of 120 mm, width of 80mm, and height of 135 mm (1.3L), which was submerged in a thermostatic water bath (42L) with a temperature adjusted range of 5-80°C. The bulk temperature of FC-72 within the test chamber was maintained at a prescribed temperature by controlling the water temperature inside the water bath. Additional liquid temperature control was provided by an internal condenser, which was attached at the ceiling of the test vessel and through which water was circulated from cooling unit. The pressure inside the test vessel was measured by pressure gauge and a nearly atmospheric pressure was maintained by attaching a rubber bag to the test vessel. For the visual observation of boiling phenomena, the test chamber was fitted with glass windows in both the front and back. The test heater assembly consisting of a test chip bonded on a pyrex glass plate and a vacuum chuck made of brass was immersed horizontally in the test chamber with the test chip facing upward. The local temperatures of the test liquid at the chip level, and 40mm and 80mm above the chip level were measured by T-type thermocouples the hot junctions of which were located on a vertical line 25mm apart from the edge of test chip.

Details of the test section are shown in Fig. 5. The test chip was a P doped N-type silicon chip with the dimensions of $10\times10\times0.5mm^3$. The specific resistance of the test chip was 1-$2\Omega cm$, and the thermal conductivity was about 156W/m.K at room temperature.
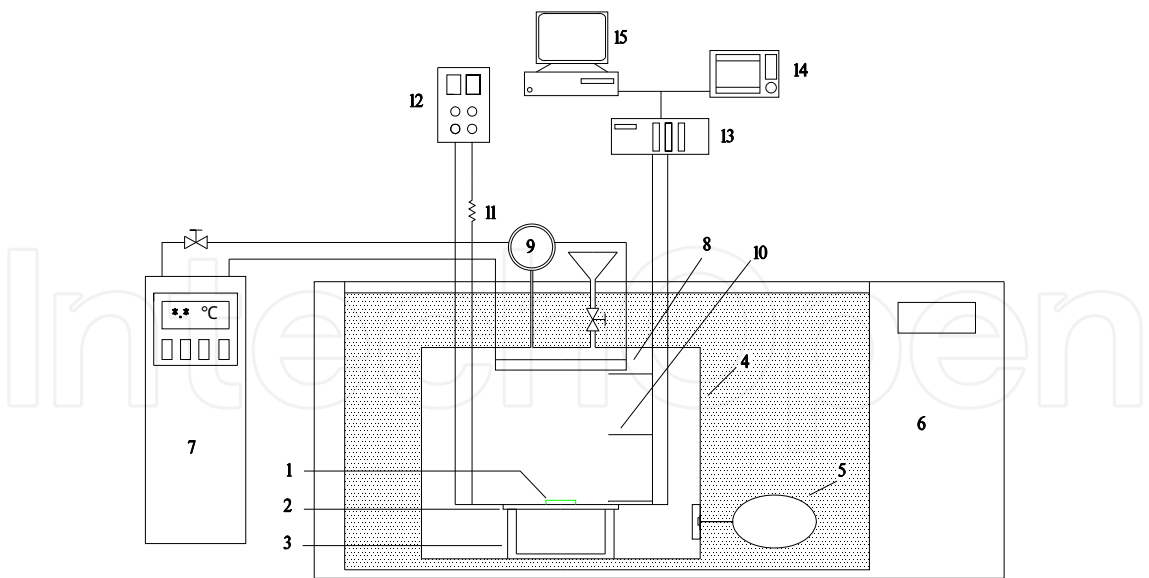
1, Test chip; 2,Glass plate; 3,Vacuum chuck; 4, Test vessel; 5,Rubber bag; 6,Water bath; 7,Cooling unit; 8, Condenser; 9,Pressure gauge; 10,Thermocouples; 11, Standard resistance; 12, DC power supply; 13, Digital multimeter; 14,Imange acquisition System; 15, Computer

Fig. 4. Schematic diagram of experimental apparatus for pool boiling
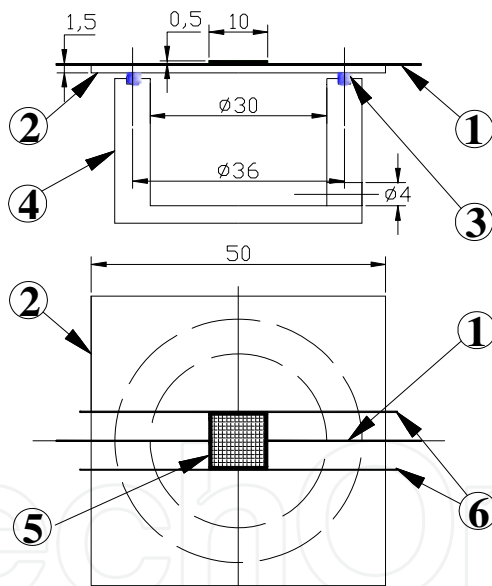
1, Thermocouple; 2, Pyrex glass plate; 3, O-ring; 4, Vacuum chuck; 5, Silicon chip;
6, Copper lead wire

Fig. 5. Test section for pool boiling

The chip was Joule heated by a direct current. Two 0.25-mm diameter copper wires for power supply and voltage drop measurement were soldered with a low temperature solder to the side surfaces at opposite ends. In order to secure the Ohmic contact between the test chip and the copper wire, a special solder with the melting point of 300°C was applied to the chip with ultrasonic bonding method before soldering the copper wires.

The local wall temperatures at the center and about 1.5mm from the edge on the centreline of the chip were measured by two 0.12-mm diameter T-type thermocouples bonded under

the test chip. The test chip was bonded on the top of a 50×50×1.2 mm³ pyrex glass plate using epoxy. Then the glass plate on which the test chip was bonded was pressed firmly to the O-ring on a brass vacuum chuck when the inside of the chuck was evacuated by using a vacuum pump. This facilitated an easy exchange of the test chip and minimization of conduction heat loss due to conduction and convection from the rear surface of the chip. The side surfaces of the chip were covered with an adhesive to minimize heat loss. Therefore, only the upper surface of the chip was effective for heat transfer.

2.2 Test facility of forced flow boiling

The second test facility for the forced flow boiling heat transfer is shown schematically in Fig. 6. It is a closed-loop circuit consisting of a tank, a scroll pump, a test section, two heat exchangers and a turbine flowmeter. The tank served as a fluid reservoir and pressure regulator during testing.
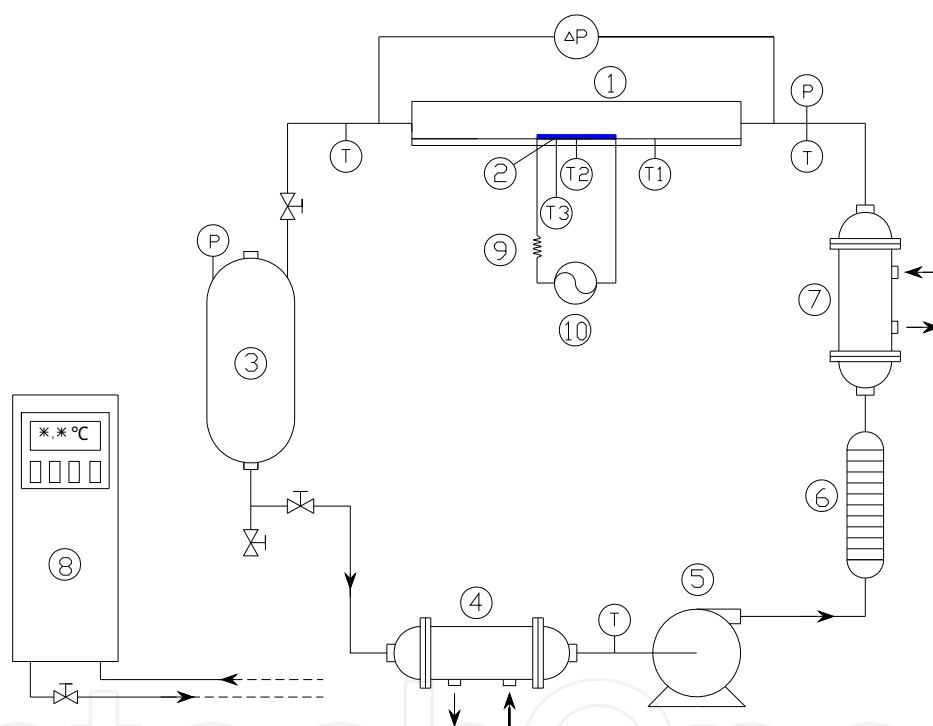

1, Test Section; 2, Test chip; 3, Tank; 4, Condenser; 5, Pump; 6, Flowmeter; 7, Pre-heater; 8, Cooling unit; 9, Standard resistance; 10, Direct current

Fig. 6. Forced flow boiling test loop

The condenser prior to the pump was used to cool the fluid and prevent cavitation in the pump. The pre-heater prior to the test section was used to control the test section inlet temperature. The pump was combined with a converter to control the mass flow rate. To ensure proper inlet pressure control, a pressure transducer was installed at the inlet of the test section. The pressure drop across the test section was also measured by a pressure difference transducer. The flowmeter and the sensors for pressure and pressure difference have the function of outputting 4~20mA current signals and were measured directly by a data acquisition system.

The test silicon chip is bonded to a substrate made of polycarbonate using epoxy adhesive and fixed in the horizontal, upward facing orientation on the bottom surface of a 5mm high

and 30mm wide horizontal channel as shown in Fig. 7. The chip is located 300mm from the inlet of the test section so that the fluid flow on it is estimated to be fully developed turbulent flow for the present fluid velocity range.
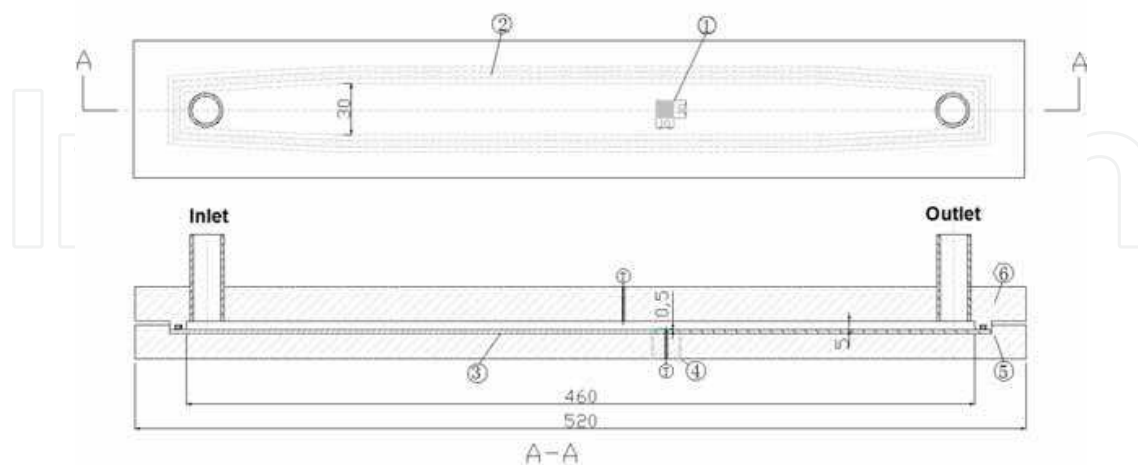
1, Test chip; 2, O-ring; 3, Polycarbonate plate; 4, Lead wires; 5, Lower cover; 6, Upper cover

Fig. 7. Test section for forced flow boiling

2.3 Experimental conditions and test procedure

Experiments were performed at three fluid velocities of 0.5, 1 and 2m/s for the second test system and the liquid subcoolings of 3, 15, 25, 35 and/or 45K for both of test systems. Six kinds of silicon chips, one with a smooth surface and five with square micro-pin-fins having fin dimensions of 30×60, 30×120, 30×200, 50×60 and 50×120 μm² (thickness×height) are tested. The fin pitch p was twice the fin thickness. The micro-pin-finned chip was fabricated by the dry etching technique. These chips were named chips S, PF30-60, PF30-120, PF30-200, PF50-60 and PF50-120, respectively. The scanning electron microscope (SEM) images of the five micro-pin-finned chips are shown in Fig. 8a-e, respectively. A smooth chip was also tested for comparison.

In the above two test systems, the test chips were Joule heated by using a programmable d.c. power supply. The power supply was connected in series to a standard resistance (1Ω) and the test chip. The standard resistance was used to measure the electric current in the circuit. Power input to the test chip was increased in small steps up to the high heat flux region of nucleate boiling. The heat flux q was obtained from the voltage drop of the test chip and the electric current. In order to prevent real heater burnout, an overheating protection system was incorporated in the power circuit. If the wall temperature sharply increases by more than 20K in a short time, the data acquisition algorithm assumed the occurrence of CHF condition and the power supply was immediately shut down. The CHF value was computed as the steady state heat flux value just prior to the shut down of the power supply. The uncertainties in the chip and bulk liquid temperature measurements by the thermocouple and the resistance thermometry for the pool boiling is estimated to be less than 0.1K and that to be less than 0.3K for the forced flow boiling. The uncertainty in the calculated value of q for the pool boiling is mostly due to the heat loss and estimated to be less than 15 and 5.0 percents for natural convection and nucleate boiling regions, respectively. For the forced flow boiling, the uncertainty in the calculated value of q is

estimated to be less than 16 and 6.0 percents for the forced convection and nucleate boiling regions respectively. It is relevant to note here that q includes the heat transferred to the bulk liquid by conduction through the copper lead wires and the polycarbonate substrate.
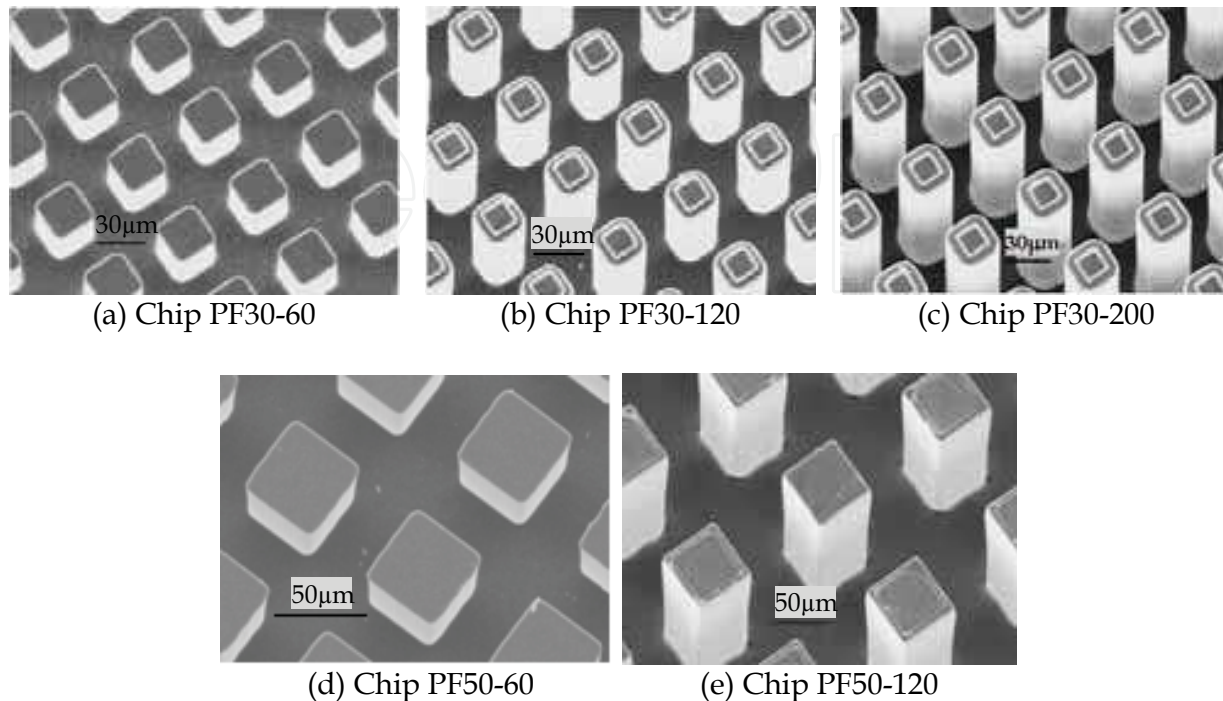

(a) Chip PF30-60   (b) Chip PF30-120   (c) Chip PF30-200

(d) Chip PF50-60   (e) Chip PF50-120

Fig. 8. SEM Images of micro-pin-fins

The experiment was repeated two or three times for all chips. The time interval between the subsequent runs was greater than 0.5 h. The boiling curves showed a good repeatability for all cases except for the boiling incipience point. Thus, only the results for the third runs are presented in the next section.

3. Results and discussion

3.1 Pool boiling performance of micro-pin-finned surfaces

Figure 9 shows the boiling curves of micro-pin-finned surfaces of PF30-60 (fin thickness of 30μm and height of 60μm) and PF30-200 (fin thickness of 30μm and height of 200μm) at $\Delta Tsub$=3K. The boiling curve of the smooth surface chip S is also shown for comparison. All chips follow almost the same q versus ΔT_{sat} relation in the non-boiling region despite that chip PF30-200 has a large fin height of 200 μm. This indicates that the fin height up to 200 μm is not effective in the enhancement of natural convection heat transfer. However, at the nucleate boiling region, the micro-pin-finned surfaces show considerable heat transfer enhancement compared to chip S. Furthermore, the boiling curves of chips PF30-60 and PF30-200 are very steep and the wall superheats show a very small change with increasing heat flux q up to the critical heat flux (CHF) point. It is supposed that the increased surface activated in the nucleate region to be much larger for chips PF30-60 and PF30-200, hence the boiling heat transfer is enhanced more greatly. The q_{CHF} increases in the order of chips S, PF30-60 and PF30-200. For the micro-pin-finned chips in the present study, the wall temperature at the CHF point is lower than 85°C.
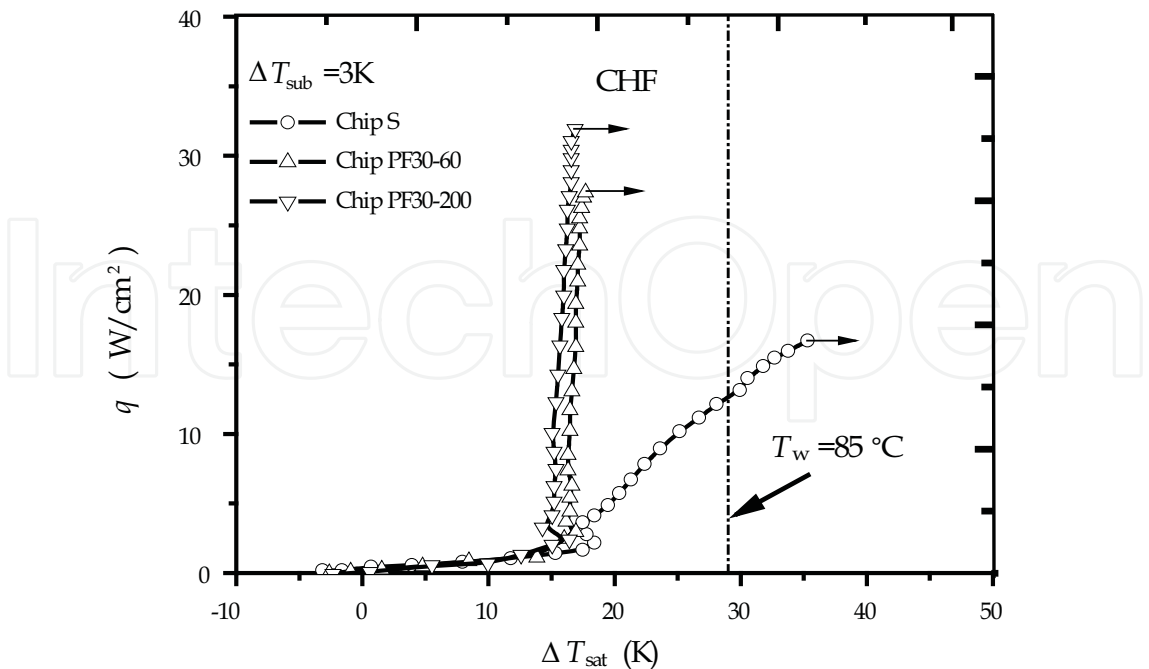
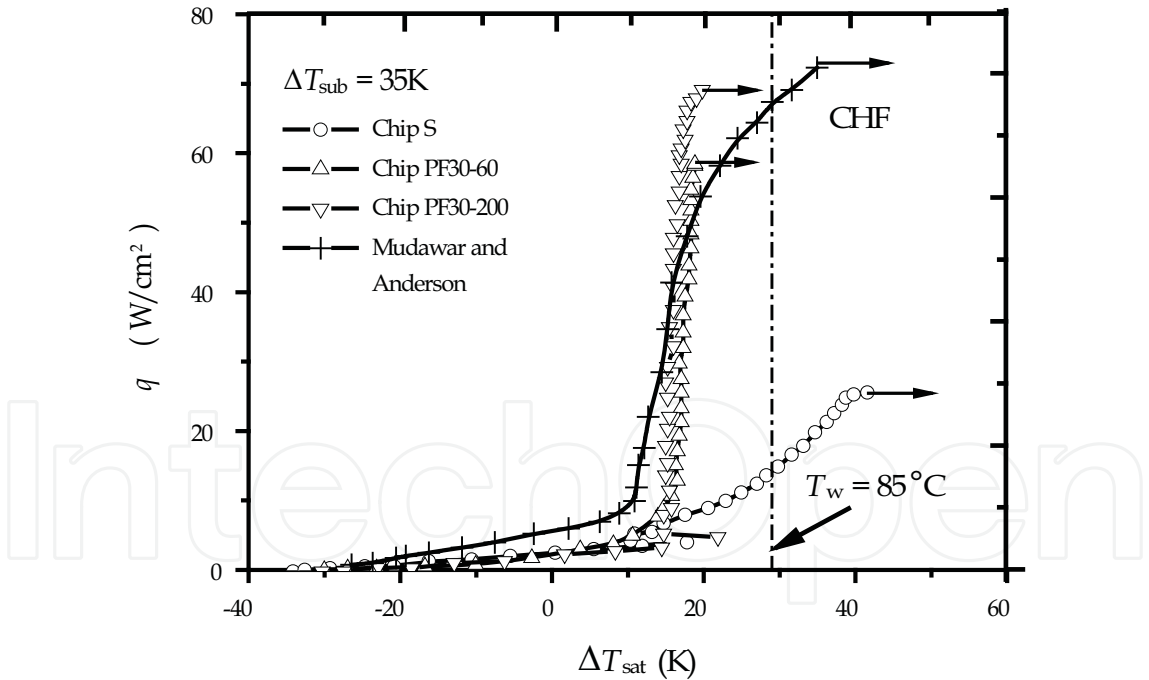Fig. 9. Boiling curves of chips PF30-60, PF30-200 and S, ΔT_{sub}=3K

Fig. 10. Boiling curves of chips PF30-60, PF30-200 and S, ΔT_{sub}=35K

Figures 10 and 11, respectively, show the boiling curves of micro-pin-finned chip PF30-60 and PF30-200 at ΔT_{sub}=35K and ΔT_{sub}=45K. In Fig. 10, the boiling curves of the micro-pin-finned surface reported by Mudawar and Anderson (1989) and a smooth surface are also shown for comparison. The test surface of Mudawar and Anderson (1989) had square micro-pin-fins with the dimensions of 0.305×0.508 mm² (thickness×height). These fin dimensions

are one order of magnitude greater than those of chip PF30-60 in the present experiments. The $\varDelta T_{sat}$ values in the low-heat-flux region are smaller than that for chips PF30-60 and PF30-200, whereas the wall superheats at the CHF point $\varDelta T_{sat,CHF}$ are greater than that for the latter. While the measured heat flux in the free convection region for chip S and the micro-pin-finned chips in this study is almost the same, the heat flux for the micro-pin-finned chip reported by Mudawar and Anderson (1989) is about 40% higher than that for chip S, indicating that the increased area of their micro-pin-finned surface over a smooth surface is effective in natural convection heat transfer.
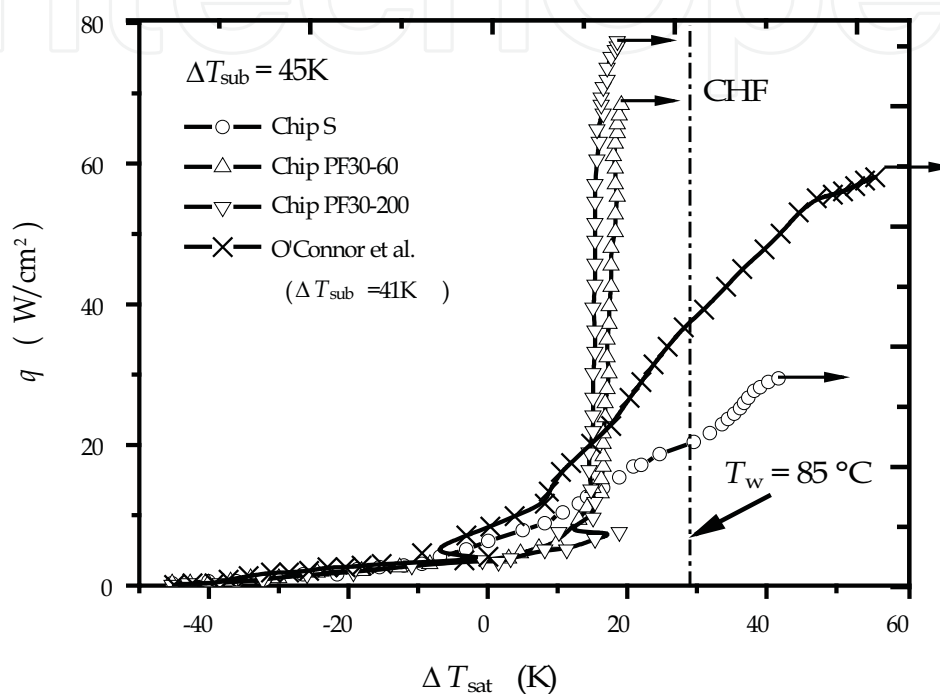

Fig. 11. Boiling curves of chips PF30-60, PF30-200 and S, $\varDelta T_{sub}$=45K

Although the q_{CHF} reported by Mudawar and Anderson (1989) for the micro-pin-finned surface is higher than that of chips PF30-60 and PF30-200, the boiling curve near the CHF point shows a much smaller slop than the micro-pin-finned chips in the present study.

In Fig. 11 boiling occurs at a much smaller value of $\varDelta T_{sat}$ and the temperature overshoots at the boiling incipience are small, compared to the case of Fig. 10. The boiling curves of the microporous surface developed by O'Connor et al. (1996) and a smooth surface are also shown for comparison. The test surface of O'Connor et al. (1996) had a porous layer consisting of 8-12 μm diamond particles produced by painting technique. The porous surface shows a severe deterioration of boiling heat transfer performance at high heat flux region and the value of q_{CHF} is smaller than that of the micro-pin-finned chips. However, the micro-pin-finned surfaces in the present study show a sharp increase in the heat flux with increasing wall superheat from the boiling incipience to the critical heat flux. The increase of CHF for micro-pin-finned surfaces could reach more than twice that of a smooth chip. Comparison of the experimental results reveals that the wall temperature at the CHF point $T_{w,CHF}$ is higher than 85°C for chip S and the previous results reported by Mudawar and Anderson (1989) and O'Connor et al. (1996). On the other hand, the micro-pin-finned chips PF30-60 and PF30-200 show $T_{w,CHF}$ smaller than 85°C.

As stated previously, the upper limit of temperature for a reliable operation of electronic chips is given by 85°C. Thus the maximum allowable heat flux q_{max} is given by the CHF if $T_{w,CHF}$<85°C and by q at T_w=85°C if $T_{w,CHF}$>85°C. Figure 12 shows the variation of maximum heat flux of chips PF30-60 and PF30-200 with liquid subcooling ΔT_{sub}. The experimental data by Mudawar and Anderson (1989) and O'Connor et al (1996) are also shown for comparison. We can see that the maximum heat flux of the micro-pin-finned surfaces in the present study is much higher than that of the porous and other large scale micro-pin-finned and smooth surfaces, and increases greatly with the liquid subcooling. The micro-pin-finned surface of Mudawar and Anderson (1989) shows almost the same q_{max} with chip PF30-200. The porous surface of O'Connor et al (1996) shows the q_{max} value in between those for micro-pin-finned chips and smooth chip. The difference of q_{max} between the porous surface and micro-pin-finned surfaces increases greatly with subcooling, indicating that the subcooling effect is larger for the micro-pin-finned surfaces.
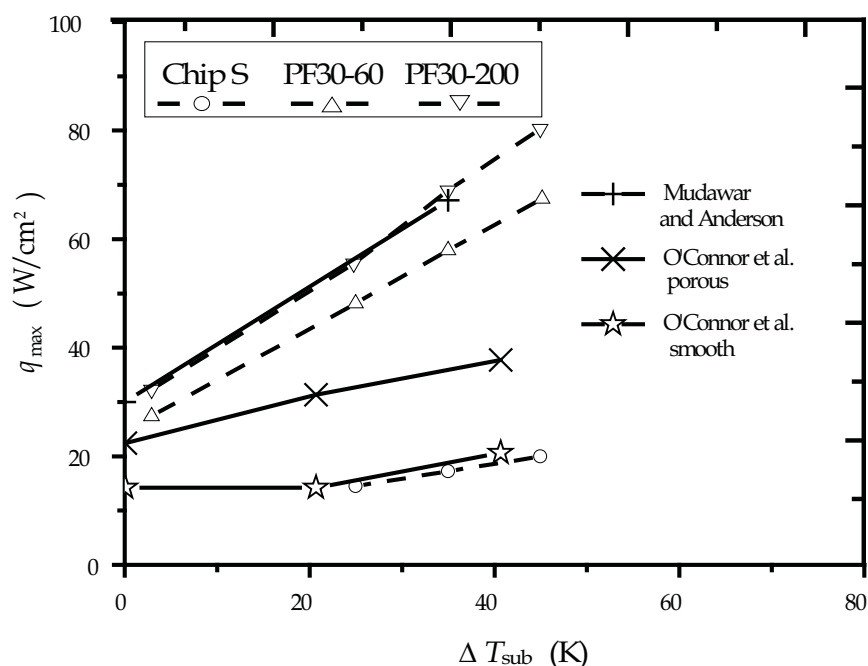

Fig. 12. Variation of q_{max} with ΔT_{sub}

3.2 Flow boiling performance of micro-pin-finned surfaces

Figure 13 shows the comparison of boiling curves for all surfaces with ΔT_{sub}=15K. For the fluid velocity V<2m/s, the wall superheat in the nucleate boiling region decreases in the order of chip S, PF50-60, PF30-60, PF30-120 for the same fluid velocity, again showing that the boiling heat transfer can be enhanced by increasing total surface area. However, the boiling curve of chip PF50-120 shows the smallest wall superheat despite of the surface area ratio of 3.4. Although the condition for the etching process is set to the same, the etching size is different for different micro-pin-finned chips, which may affect the etching results. From the scanning-electron-micrograph (SEM) image of micro-pin-fin (Fig. 8), we found that the roughness on the fin flank near the fin root usually increases with increasing etching depth. Chip PF50-120 with the largest fin thickness and height is observed to have a large roughness scale on the fin flank. It is considered that the roughness causes the earlier boiling incipience and thus smaller wall superheat in the nucleate boiling region. For the fluid

velocity of 2m/s, the nucleate boiling curves of all micro-pin-finned chips are more or less affected by forced convection heat transfer since the slopes of boiling curves become smaller than those at lower velocities, but the nucleate boiling curves of 50-μm thick micro-pin-fins show a much larger slope than those of 30-μm thick micro-pin-fins. According to enhanced boiling heat transfer mechanism for micro-pin-fins developed by Wei et al. (2003), the microlayer evaporation and the Marangoni convection caused by thermal capillary force in the micro-pin-fin formed interconnect tunnel play an important role for boiling heat transfer. It is considered that bulk fluid flow may affect the Marangoni convection greatly and the smaller fin gap of 30 μm may generate a larger flow resistance for Marangoni convection around the fin sidewalls, resulting in a lower heat transfer performance. The larger slope shifts the boiling curve of chips PF50-60 and PF50-120 to a smaller wall superheat than that of chips PF30-60 and PF30-120, respectively, at high heat flux for V=2m/s. For comparison, Lie et al. (2007)'s saturated boiling curves for two pin-finned surfaces with the larger fin thicknesses of 100 and 200 μm are also shown in Fig. 13.
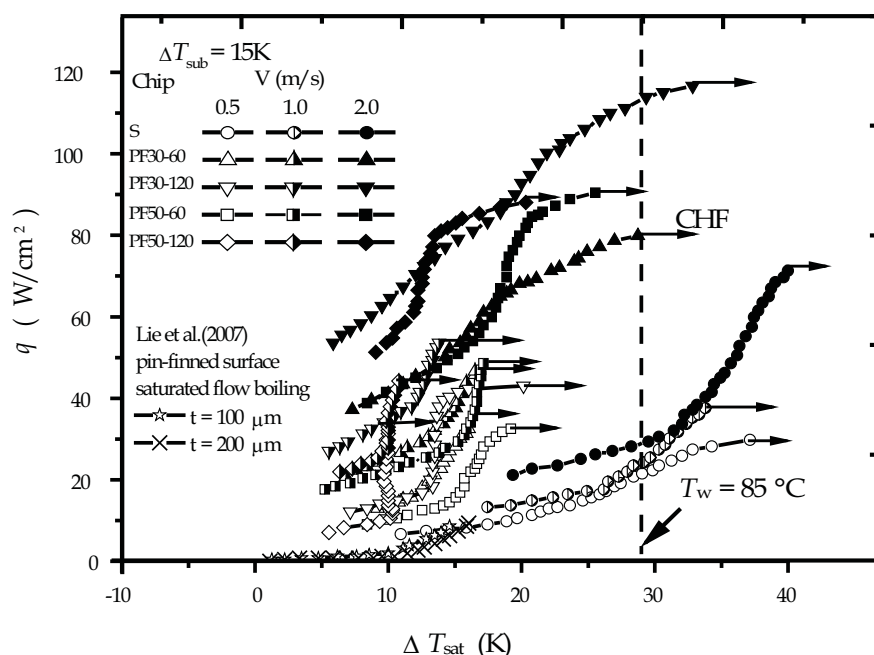

Fig. 13. Comparison of flow boiling curves for all chips, ΔT_{sub}=15K

The boiling curves of Lie et al. (2007) show a much smaller slope and a larger wall superheat compared with that of the present micro-pin-finned surfaces. Generally, the wall superheat deceases in the order of 200, 100, 50 and 30-μm micro-pin-fins for the fin height of about 70μm. We have found that the boiling heat transfer performance for the micro-pin-finned surface with the fin thickness of 10-50 μm is much better than the pin-finned surface with the larger fin thickness of about 300 μm used by Anderson and Mudawar (1989), and the fin thickness of 30-50μm is a suitable range of effectively enhancing boiling heat transfer. The optimum fin gap size is considered to be determined by the balance of the capillary force caused by evaporation of bubbles for driving the micro-flow in the gap of micro-pin-fins and the flow resistance. Large fin gap usually has small flow resistance but generates small microconvection heat transfer proportion, and *vice versa*. The present experimental study again shows the larger fin thickness above 100 μm is not so remarkably effective compared with the fin thickness of 30-50 μm.

Figures 14 and 15 show the comparison of boiling curves for all surfaces with ΔT_{sub}=25 and 35K, respectively. The trend of experimental data is basically the same as the case of ΔT_{sub}=15K shown in Fig. 13 except that the values of the CHF increase considerably in the order of 25 and 35 K.
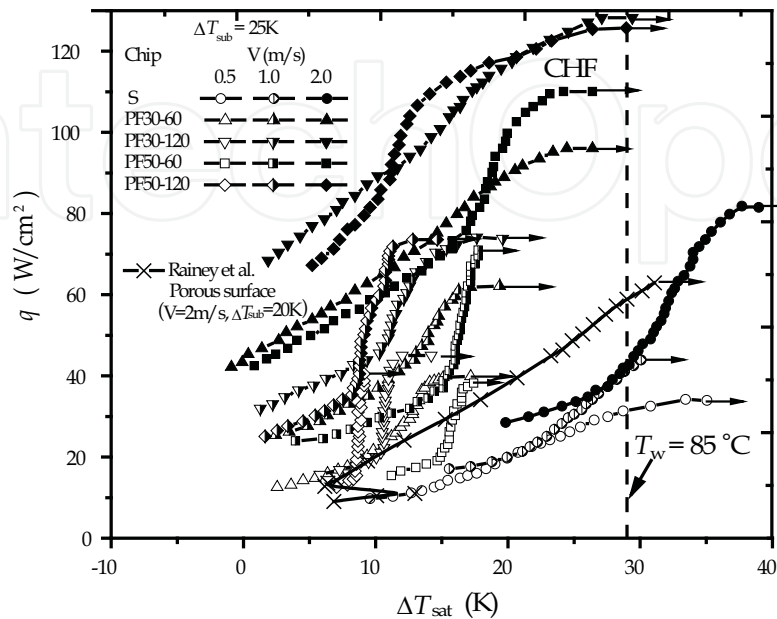

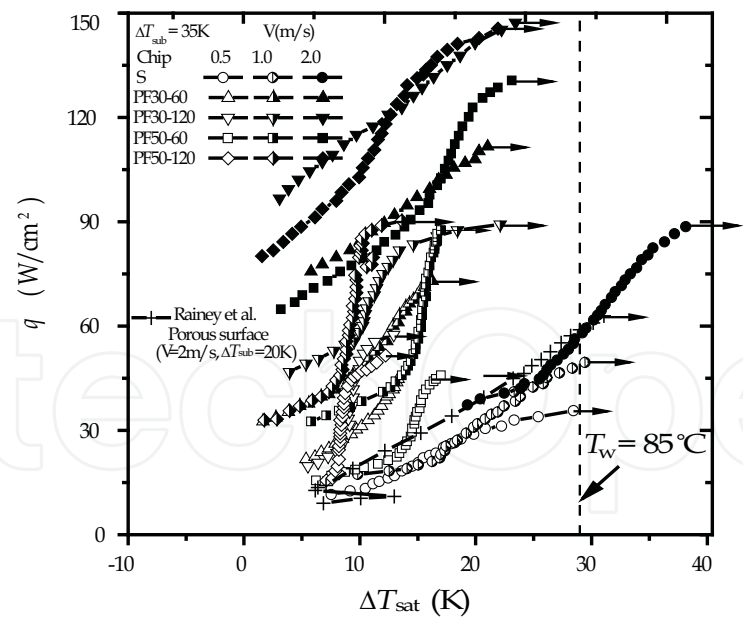Fig. 14. Comparison of flow boiling curves for all chips, ΔT_{sub}=25K

Fig. 15. Comparison of flow boiling curves for all chips, ΔT_{sub}=35K

The highest value of CHF (=148 W/cm²), about 1.5 times as large as that for the smooth surface, was obtained by chips PF30-120 (fin thickness of 30 μm and height of 120 μm) and PF50-120 (fin thickness of 50 μm and height of 120 μm) at liquid subcooling ΔT_{sub} = 35 K and flow velocity V = 2 m/s. For comparison, Rainey et al.(2001) 's boiling curve with the liquid subcooling of 20 K for the microporous surface at V = 2 m/s is also shown in Figs. 14

and 15. Although having an earlier boiling incipience, the microporous surface shows a larger wall superheat than the micro-pin-finned surfaces in the nucleate boiling region, and the heat flux at 85°C is less than half the CHF of chips PF30-120 and PF50-120.

We plot the relation ship of q_{max} with fluid velocity for all surfaces with fluid subcooling as a parameter in Fig. 16. The fluid velocity has a very large effect on q_{max}. For the low fluid subcooling of 15K and the velocity larger than 1m/s, the rate of q_{max} enhancement is increased remarkably, which was also supported by many researches such as Mudawar and Maddox (1989), Rainey et al. (2001), and etc., who had noted that the transition from low to high velocities was characterized by an increase in the rate of CHF enhancement with velocity. However, for the larger liquid subcoolings of 25 and 35K, the transition from low to high velocity is characterized by a decrease in the rate of q_{max} enhancement with velocity.
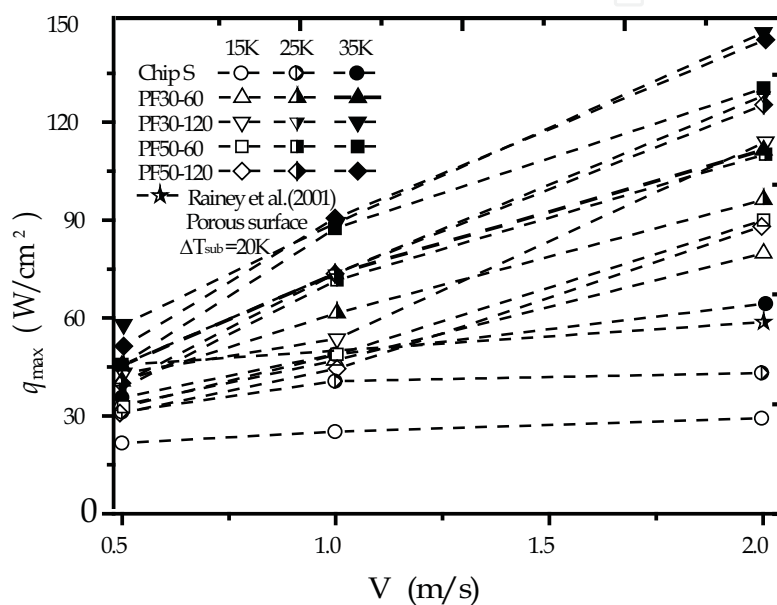

Fig. 16. Effects of fluid velocities and subcoolings on CHF

For a low fluid subcooling, as explained by Mudawar and Maddox (1989), the low velocity q_{max} was caused by dryout of the liquid sublayer beneath a large continuous vapor blanket near the downstream edge of the heater; however in the high velocity q_{max} regime, the thin vapor layer covering the surface was broken into continuous vapor blankets much smaller than the heater surface, decreasing the resistance of fluid flow to rewet the liquid sublayer and thus providing an additional enhancement to q_{max} and subsequent increase in slope. For a large fluid subcooling, the bubble size becomes small and the heater surface was not fully occupied with vapor layer for the fluid velocity range in this study. Therefore, there is no obvious slope change as seen in Fig. 16. Moreover, from the slope of boiling curves we can see that the effect of the fluid velocity on micro-pin-finned surfaces is more noticeably compared with the porous surface (Rainey et al. 2001) and the smooth surface, and the enhancement of q_{max} sharply increases with fluid velocity. For chips PF30-120 and PF50-120, the q_{max} reaches nearly 148W/cm² at V=2m/s and ΔT_{sub}=35K.

4. Conclusions and future research

All micro-pin-fined surfaces have considerable heat transfer enhancement compared with a smooth surface and other microstructured surfaces, and the maximum CHF can reach

nearly 148W/cm² by chips PF30-120 and PF50-120 at V= 2 m/s and ΔT_{sub} = 35 K. The wall temperature for the micro-pin-finned surfaces is less than the upper temperature limit for the normal operation of LSI chip, 85°C. Therefore, micro-pin-finned surfaces are very prospective for high-efficiency electronic cooling.

Electronics cooling by using boiling heat transfer in space and on planetary neighbors has become an increasing significant subject. For the boiling heat transfer in microgravity, the buoyancy effect becomes weak, resulting in a longer stay time for the bubble departure. These may prevent the effective access of fresh bulk liquid to the heater surface in time, resulting in a lower boiling heat transfer performance at high heat flux (Wan and Zhao 2008). How to improve boiling heat transfer effectively in microgravity is an important issue. According to the excellent boiling heat transfer performance of the micro-pin-finned surfaces and the enhanced boiling heat transfer mechanism, it is supposed that although the bubbles staying on the top of the micro-pin-fins can not be detached soon in microgravity, the fresh bulk liquid may still access to the heater surface through interconnect tunnels formed by the micro-pin-fins due to the capillary forces, which is independent of the gravity level. Therefore, it is our great interest to study the boiling heat transfer performance of micro-pin-finned surfaces in microgravity in the future.

5. Acknowledgement

6. References

Anderson, T.M. & Mudawar, I. (1989). Microelectronic cooling by enhanced pool boiling of a dielectric fluorocarbon liquid. ASME J. Heat Transfer, 111:752-759

Bergles, A.E. & Chyu, M.C. (1982). Characteristics of nucleate pool boiling from porous metallic coatings. ASME J. Heat Transfer, 104:279-285

Chang, J.Y. & You, S.M. (1996). Heat orientation effects on pool boiling of micro-porous-enhanced surfaces in saturated FC-72. ASME J. Heat Transfer, 118:937-943

Chang, J.Y. & You, S.M. (1997). Enhanced boiling heat transfer from micro-porous surfaces: effects of a coating composition and method. Int. J. Heat Mass Transfer, 40:4449-4460

Chowdhury, S.K.R. & Winterton, R.H.S. (1985). Surface effects in pool boiling. Int. J. Heat Mass Transfer, 28:1881-1889

Chu, R.C. & Moran, K.P. (1977). Method for customizing nucleate boiling heat transfer from electronic units immersed in dielectric coolant. US Patent 4,650,507

El-Genk, M.S. & Ali, A.F. (2010). Enhancement of saturation boiling of PF-5060 on microporous copper dendrite surfaces. ASME J. Heat Transfer, 132:071501(1-9)

Hwang, U.P. & Moran, K.F. (1981). Boiling heat transfer of silicon integrated circuits chip mounted on a substrate. In: ASME HTD, 20:53-59

Kitching, D.; Ogata, T. & Bar-cohen, A. (1995). Thermal performance of a passive immersion cooling multichip module. J. Enhanced Heat Transfer, 2:95-103

Kubo, H.; Takamatsu, H. & Honda, H. (1999). Effects of size and number density of micro-reentrant cavities on boiling heat transfer from a silicon chip immersed in degassed and gas-dissolved FC-72. Enhanced Heat Transfer, 6:151-160

Kutateladze,S.S. & Burakov, B.A. (1989).The critical heat flux for natural convection and forced flow of boiling and subcooled dowtherm. Problems of Heat Transfer and Hydraulics of Two-Phase Media, Pergamon,Oxford, pp. 63–70

Li, S.; Furberg, R.; Toprak, M.S.; Palm, B. & Muhammed, M. (2008). Nature-inspired boiling enhancement by novel nanostructure macroporous surfaces. Adv. Funct. Mater., 18:2215-2220

Lie, Y.M.; Ke, J.H.; Chang, W.R.; Cheng, T.C. & Lin, T.F. (2007). Saturated flow boiling heat transfer and associated bubble characteristics of FC-72 on a heated micro-pin-finned silicon chip. Int. J. Heat Mass Transfer, 50:3862-3876

Messina, A.D.; & Park, E.L. (1981). Effects of precise arrays of pits on nucleate boiling. Int. J. Heat Mass Transfer, 24:141-145

Mudawar, I. & Anderson, T.M. (1989). High flux electronic cooling by means of pool boiling – Part I; parametric investigation of the effects of coolant variation, pressurization, subcooling and surface sugmentation. Heat Transfer Electron ASME-HTD, 111:25-34

Mudawar,I. & Maddox,D.E. (1989). Critical heat flux in subcooled flow boiling of fluorocarbon liquid on a simulated electronic chip in a vertical rectangular channel. Int. J. Heat and Mass Transfer, 32: 379–394.

Nakayama, W.; Nakajima, T.; Ohashi, S. & Kuwahara, H. (1989). Modeling of temperature transient of micro-porous studs in boiling dielectric fluid after stepwise power application. ASME HTD, 111:17-23

Nelson, L.A.; Sekhon, K.S.; & Fritz, J.E. (1978). Direct heat pipe cooling of semiconductor devices. In: Proceedings of the 3rd international heat pipe conference, CA, USA, pp.373-376

Nakayama, W.; Daikoku, T. & Nakajima, T. (1982). Effects of pore diameters and system pressure on saturated pool nucleate boiling heat transfer from porous surfaces. ASME J. Heat Transfer, 104:286-291

O'Connor, J.P. & You, S.M. (1995). A painting technique to enhance pool boiling heat transfer in saturated FC-72. ASME J. Heat Transfer, 117:387-393

O'Connor, J.P.; You, S.M. & Chang, J.Y. (1996). Gas saturated pool boiling heat transfer from smooth and microporous surfaces in FC-72. ASME J. Heat Transfer, 118:662-667

Oktay, S. (1982). Departure from natural convection (DNC) in low-temperature boiling heat transfer encountered in cooling microelectronic LSI devices. In: Proc. 7th Int. Heat transfer Conf., 4:113-118

Oktay, S. & Schmeckenbecher, A. (1972). A method for forming heat sinks on semiconductor device chips. US Patent 3,706,127

Phadke, N.K.; Bhavnani, S.H.; Goyal, A.; Jaeger, R.C. & Goodling, J.S. (1992). Re-entrant caviy surface enhancements for immersion cooling of silicon multichip packages. IEEE Trans. Comp., Hybrids, Manuf. Technol.,15:815-822

Rainey, K.N.; Li, G. & You, S.M. (2001). Flow Boiling Heat Transfer From Plain and Microporous Coated Surfaces in Subcooled FC-72. ASME J. Heat Transfer, 123(5): 918-925

Samant, K.R. & Simon, T.W. (1989). Heat transfer from a small heatedregion to R-113 and FC-72. ASME J. Heat Transfer, 111:1053–1059

Ujereh, S.; Fisher, T.; & Mudawar, I. (2007). Effects of carbon nanotube arrays on nucleate pool boiling. Int. J. Heat Mass Transfer, 50:4023-4038

Wan, S.X. & Zhao, J.F. (2008). Pool boiling in microgravity: recent results and perspectives for the project DEPA-SJ10. Microgravity Sci. Technol., 20:219-224

Wei, J.J.; Yu, B. & Wang, H.S. (2003). Heat transfer mechanisms in vapor mushroom region of saturated nucleate pool boiling. Int. J. Heat and Fluid Flow, 24:210-222

You, S.M.; Simon, T.W. & Bar-Cohen, A. (1992). A technique for enhancing boiling heat transfer with application to cooling of electron equipment. IEEE Trans CHMT, 15:823-831
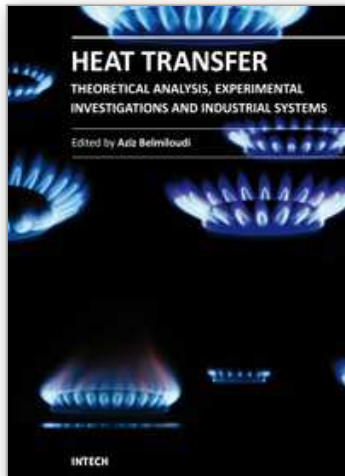
Heat Transfer - Theoretical Analysis, Experimental Investigations and Industrial Systems

Edited by Prof. Aziz Belmiloudi

Over the past few decades there has been a prolific increase in research and development in area of heat transfer, heat exchangers and their associated technologies. This book is a collection of current research in the above mentioned areas and discusses experimental, theoretical and calculation approaches and industrial utilizations with modern ideas and methods to study heat transfer for single and multiphase systems. The topics considered include various basic concepts of heat transfer, the fundamental modes of heat transfer (namely conduction, convection and radiation), thermophysical properties, condensation, boiling, freezing, innovative experiments, measurement analysis, theoretical models and simulations, with many real-world problems and important modern applications. The book is divided in four sections : "Heat Transfer in Micro Systems", "Boiling, Freezing and Condensation Heat Transfer", "Heat Transfer and its Assessment", "Heat Transfer Calculations", and each section discusses a wide variety of techniques, methods and applications in accordance with the subjects. The combination of theoretical and experimental investigations with many important practical applications of current interest will make this book of interest to researchers, scientists, engineers and graduate students, who make use of experimental and theoretical investigations, assessment and enhancement techniques in this multidisciplinary field as well as to researchers in mathematical modelling, computer simulations and information sciences, who make use of experimental and theoretical investigations as a means of critical assessment of models and results derived from advanced numerical simulations and improvement of the developed models and numerical methods.

How to reference

In order to correctly reference this scholarly work, feel free to copy and paste the following:

Jinjia Wei and Yanfang Xue (2011). Enhanced Boiling Heat Transfer from Micro-Pin-Finned Silicon Chips, Heat Transfer - Theoretical Analysis, Experimental Investigations and Industrial Systems, Prof. Aziz Belmiloudi (Ed.), ISBN: 978-953-307-226-5, InTech, Available from: http://www.intechopen.com/books/heat-transfer-theoretical-analysis-experimental-investigations-and-industrial-systems/enhanced-boiling-heat-transfer-from-micro-pin-finned-silicon-chips

INTECH

open science | open minds

www.intechopen.com

51000 Rijeka, Croatia
Phone: +385 (51) 770 447
Fax: +385 (51) 686 166
www.intechopen.com

中国上海市延安西路65号上海国际贵都大饭店办公楼405单元
Phone: +86-21-62489820
Fax: +86-21-62489821